Effect of Sampling Rate and Sensor Bandwidth on Measured Transient Signals in LV AC and DC Power Systems

Yljon Seferi
Institute for Energy and Environment
University of Strathclyde
Glasgow, United Kingdom
yljon.seferi@strath.ac.uk

Arshad
Institute for Energy and Environment
University of Strathclyde
Glasgow, United Kingdom
arshad.100@strath.ac.uk

Mazheruddin H. Syed
Institute for Energy and Environment
University of Strathclyde
Glasgow, United Kingdom
mazheruddin.syed@strath.ac.uk

Graeme Burt
Institute for Energy and Environment
University of Strathclyde
Glasgow, United Kingdom
graeme.burt@strath.ac.uk

Brian G. Stewart
Institute for Energy and Environment
University of Strathclyde
Glasgow, United Kingdom
brian.stewart.100@strath.ac.uk

Abstract—**Impulsive transients in power systems can stress the state of electrical insulation of equipment. Knowledge of signal characteristics is of paramount importance to accurately assess their impact on electrical insulation. This paper investigates the effect of sampling rate and sensor bandwidth on capturing high-frequency transient disturbances and their characteristics in laboratory-scale LV AC and DC systems to increase the understanding of their impact on electrical insulation. Two measurement systems of different bandwidths and configurable sampling rates, up to 500 kS/s and up to 250 MS/s, have been used in parallel to capture and compare the high-frequency transient phenomenon in voltage signals following DC series electric arc faults and the AC output of a bi-directional power converter. The presence of unknown high-frequency transient signals of magnitudes more than 10% and more than 600% with respect to the considered voltage of the system were found to exist in AC and DC recorded signals, respectively. Three dependency curves relating the maximum voltage, the rate-of-rise, and the pulse duration of the transients to different sampling rates are experimentally established to provide an improved appreciation of transient characteristics and a better correlation of their impact on the electrical insulation systems.**

Index Terms—**power quality, data acquisition, impulsive transients, electrical insulation, dielectric breakdown, partial discharge, electric arc faults**

I. Introduction

In the last few decades, there has been an increased interest in understanding the long-term and short-term impact of power quality (PQ) on AC and DC system operation [1]–[5], as well as on the ageing mechanism of electrical insulation systems [6]–[8]. The increased use of converter-connected generation and storage has introduced challenges in maintaining a certain level of PQ. The use of power electronic converters and non-linear loads can generate significant harmonics and voltage transients that affect a broad range of applications such as the operation of a protection system [9], [10], lead to malfunction of power plants [11], cause large errors in smart meter readings [12], [13], malfunction of sensitive electronic devices, and may also affect the useful service life of distribution transformers [14], [15].

The presence of long-term harmonic voltages, unbalance, and over-voltage conditions impose additional stress on the insulating dielectric material, causing cable overheating resulting in reduced useful service life [8], [16]. On the other hand, short-time events such as impulsive transients and switching surges having high frequency content lead to electrical tree inception, to an increased number of partial discharge occurrences, and usually to dielectric breakdown when the insulation state is not monitored [7], [17]–[19].

DC applications and grids are recently emerging [20]–[22], but the knowledge about PQ in DC systems and its impact on DC equipment and associated electrical insulation is currently limited. In such a context, the variety of emissions conducted from common PQ phenomena encountered on DC applications such as arc faults, short-circuits, and load changes need to be better understood. Appreciation of voltage-transient intensity and other related characteristics also requires to be better quantified to enhance the understanding of their impact on electrical insulation.

The sampling rate and sensor bandwidth impact on high-frequency transient disturbances conducted from laboratory-generated DC series electric arc faults and the AC output of a Tri-phase inverter system are investigated as part of this paper. Two measurement systems with configurable sampling rates, up to 500 kS/s and up to 250 MS/s, both employing different sensor bandwidths, are employed simultaneously to record and compare the high-frequency transient characteristics analysed. Maximum voltage, rate-of-rise, and pulse duration signal characteristics are calculated for every signal captured at different

sampling rates to represent the parameter dependency from the sampling rate of the measurement system.

The remainder of the paper is structured as follows: Section II presents AC and DC measurement setups with the experiments and methodology to analyse the data presented in Section III. Results and discussions are presented in section IV. Conclusions are summarised in Section V.

II. EXPERIMENTAL SETUP

Two separate experimental setups were used for AC and DC measurements. The AC measurements were performed at the output of a Tri-phase inverter while the DC measurements were performed across a DC series arc generator. Details about each experimental setup and the associated hardware are given in the following sections.

A. AC Experimental Setup

The AC experimental setup is shown in Fig. 1. A static load bank of 40 kW, 30 kVAR having 256 steps is connected to 90 kVA Triphase inverter. The HVPD SMART-TB3 current sensor combines low frequency and high frequency measurements in a single device. It utilizes the detection capability of the HFCT sensor to reveal high frequency disturbances and incorporates lower frequency bands for detection of power frequency (50/60 Hz), power quality, harmonics and current signature analysis (CSA). For voltage measurement at the output of Triphase, an active differential probe model Testec SI 9002 was used, capable of measuring ±1400 V (DC + peak AC) signals with a scaling factor of 200:1. The frequency bandwidth of the voltage probe is DC to 25 MHz. The voltage and current sensors are connected to a data acquisition system (DAQ) with two data acquisition cards with 8 channels each (HBM Gen2tB). The two cards have configurable sampling rates from a few samples per second to up to 25 MS/s and 250 MS/s respectively and have the ability to simultaneously measure two waveform at different sampling rates.

B. DC Experimental Setup.

Fig. 2 presents the block diagram of the DC experimental setup. The power circuit consists of a DC programmable power supply (Sorensen SGA 600X17), connected in series with an inductor and a load resistor of 4.8 Ω. Between the inductor and load resistor, an insulated controlled motorised actuator pulls apart the two copper electrodes in opposite directions under load conditions of 48 V, 10 A. The electrode motion interrupts the conducted current of the circuit and gives rise to a DC arc-fault phenomenon and a series of conducted electromagnetic disturbances comprising voltage transients.

Two measurements systems are considered for comparisons. The first is a lower sensor bandwidth and lower sampling frequency capture system. The other is a higher bandwidth sensor with higher sampling frequency capture. The first system built with off-the-shelf components includes a hall effect current transducer (LEM LA 55-P, bandwidth DC-200 kHz), a hall effect voltage transducer (LEM LV 25-P, bandwidth DC-15 kHz), and a DAQ consisting of an NI 9223 C series module from National Instruments incorporated into a compact RIO chassis. The analog-to-digital converter module can digitise up to 1 MS/s and is equipped with simultaneous sampling capability. The second measurement system comprises the differential voltage probe (Testec SI 9002); a high precision current probe (PICO TA 189) for current measurements with a bandwidth ranging from DC to 100 kHz; and the DAQ system (HBM Gen2tB) as described in the AC experimental setup.

III. METHODOLOGY

The conducted AC and DC experiments and the methodology used to compare the results are described in this section. In the case of AC experiments, the output voltages of the Triphase inverter were measured at sampling rates of (5, 10, 12.5, 25, 50, 100, 200, 250, and 500) kS/s as well as at (1, 10, 100, and 250) MS/s. The static load bank was configured at a power factor of 0.9 lagging and was kept constant throughout the experiments. The aim of this test scenario is to understand the transient phenomenon of the voltage output of the Triphase inverter. The recorded time domain signals are transformed into frequency domain, with respective frequency spectra qualitatively analysed to reveal changes in frequency spectrum with changes in sampling rate of the data acquisition system.

Two different test scenarios have been implemented in the case of the DC experiments. The first group of experiments is devoted to the detection and recording of voltage surges resulting from DC arc faults influenced by different inductors (44.3, 99.4, 236.9, 554, 2320, and 9130) μH inserted into the power circuit as indicated in Fig. 2. The choice of different
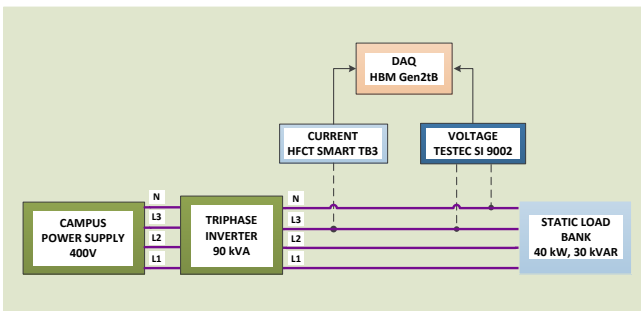

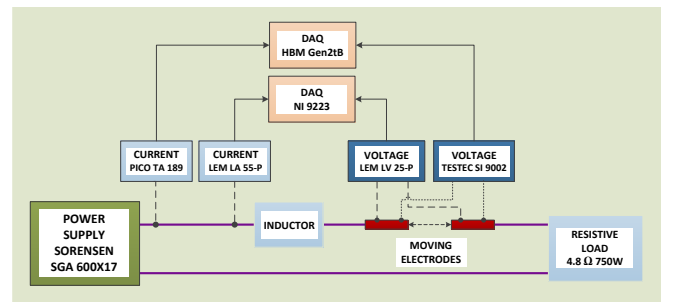Fig. 1: Schematic diagram of AC experimental setup.

Fig. 2: Schematic diagram of the DC experimental setup.

inductors emulates more realistic circuit parameters representing various converters' output filters and different cable lengths at which the arc fault can occur. The two measurement systems capture the signals simultaneously, with HBM-based DAQ measurement system configured to sample the signals at sampling rates (0.5, 1, 10, and 50) MHz, and the compact RIO-based DAQ measurement system programmed to digitise voltage and current at 500 kHz only.

The second group of experiments aims to quantitatively analyse the time domain signal characteristics of the voltage surges, and estimate dissimilarities resulting from different sampling rates of measurement systems. In this test plan, only one inductor of value 2320 μH has been used. The HBM-based DAQ measurement system has been configured to sample the signals at sampling rates of (0.1, 0.2, 0.5, 1, 2, 5, 10, 20, and 50) MHz, whereas the compact RIO-based DAQ measurement system at 500 kHz.

IV. RESULTS AND DISCUSSIONS

A. AC Measurement Results

The time domain waveform and corresponding frequency spectrums for the output voltage of triphase measured at different sampling rates are shown in Fig. 3.

It is important to note that the test conditions were kept constant and only the sampling rate was varied. It is evident from Fig. 3 that as sampling rate is increased from 5 kS/s to 500 kS/s the frequency spectrum reveals increased disturbances. The switching frequency of the Triphase inverter is 16 kHz, therefore these switching transients are repeated at high frequencies. In the case of 5 kS/s, no significant harmonics are present as the switching frequency cannot be captured at this sampling rate.
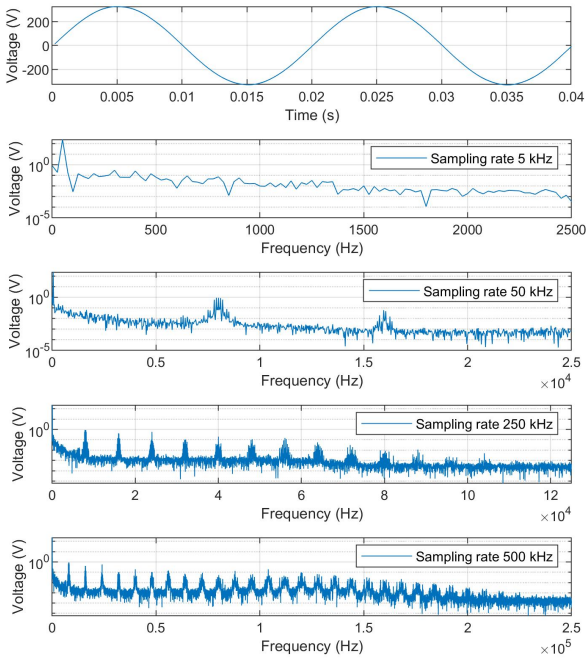

Fig. 3: Output voltage of Triphase inverter at different sampling rates.

Fig. 4 shows the half period output voltage of the Triphase measured at two sampling rates of 5 kS/s and 250 MS/s. It is evident that the high sampling rate reveals much more information as compared to the low sampling rate. For example, the repetitive transients observed in the 250 MS/s digitised signal are hidden at the 5 kS/s signal due to its limited sampling time resolution. The peak to peak measured transient amplitude is approximately 41 V and its variability with respect to the time-domain voltage recorded at 5 kS/s is ± 21 V.

B. DC Measurement Results

Laboratory generated and measured voltage surges following DC series arc phenomenon have been post-processed and presented in this subsection. The maximum surge voltage (peak voltage) of the disturbance has been considered as a metric to relate the severity of the phenomenon to the circuit parameters (size of inductor), as well as the sampling rate and bandwidth of the measurement system. Fig. 5 presents the maximum voltage observed for different inductor values placed in the circuit. The peak voltage rises with the increase of the inductor value, reaching 285.2 V or approximately 600 % more than the applied voltage of the experiment setup (48 V) for the 9130 μH inductor.

Three representative time-domain signals containing voltage transients following the DC series arcs, recorded at three different sampling rates are presented in Fig. 6. There is a clear dependence of the maximum detected voltage to the sampling rate of the measurement system. The 10 MHz sampling system can extract a maximum voltage of 4.9 times larger than the maximum transient voltage detected by the 100 kHz sampling system.

The relationship between the maximum recorded voltage and the sampling rate of the measurement system is presented in Fig. 7. The maximum voltage detected during the disturbance increases with the increase of the sampling rate. This relationship continues up to 10 MHz where the maximum recorded voltage reaches 362.4 V. A slight decrease beyond this point is observed and can be attributed to the variability and randomness nature of the DC series arcs.

The maximum detected voltage during the surges also depends upon the bandwidth of sensor used. Fig. 8 presents
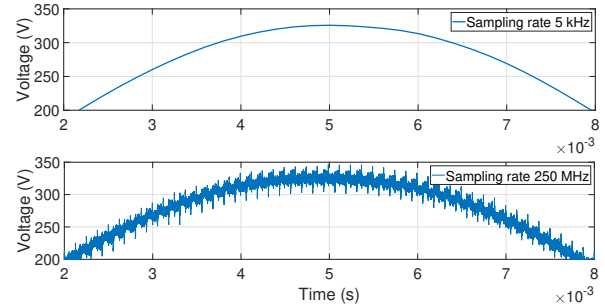

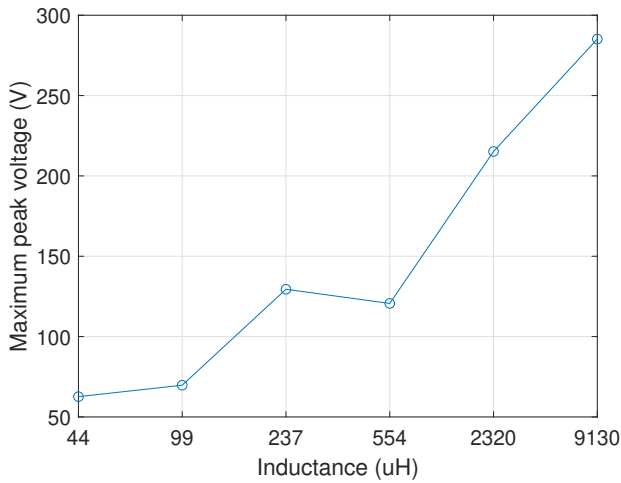Fig. 4: Comparison of voltage signals recorded at 5 kS/s and 250 MS/s.

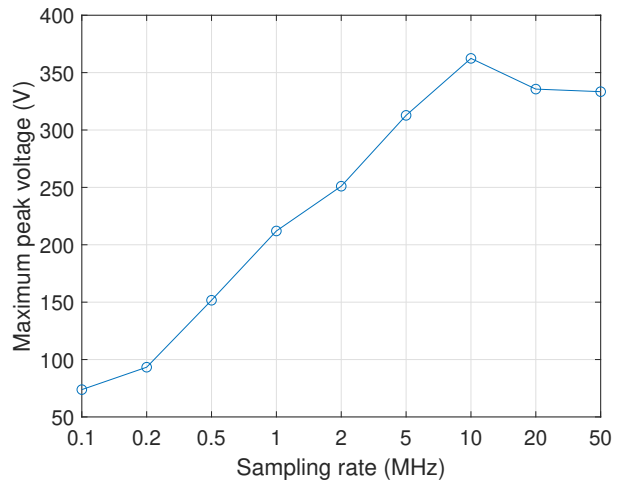Fig. 5: Peak voltage measured with different circuit inductance's.

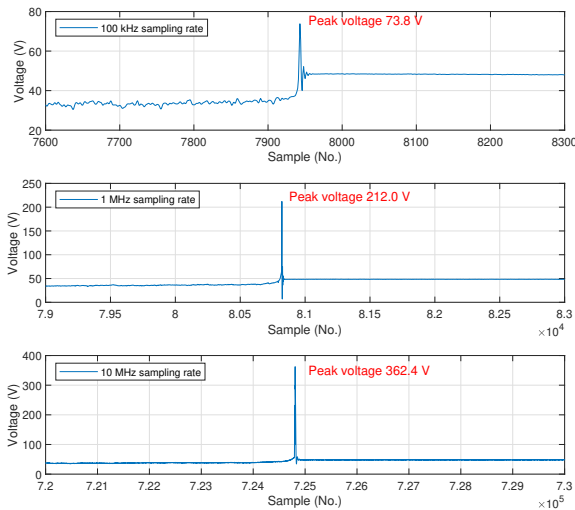Fig. 7: Peak voltage at different sampling rates.

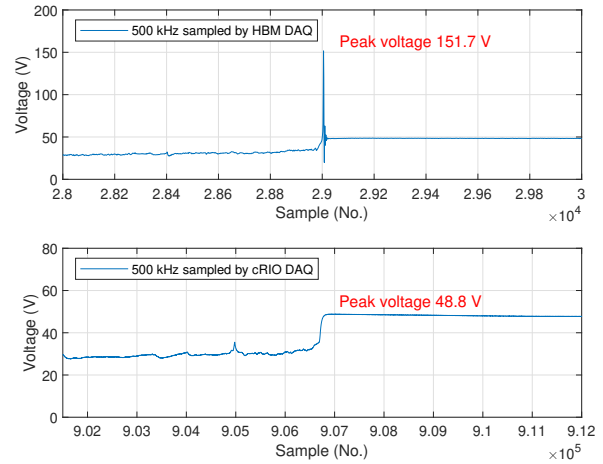Fig. 6: Captured voltage transients with varying sample rates.

Fig. 8: Signal differences between sensors bandwidths used with HBM and cRIO DAQs.

a voltage signal acquired by both DAQs at the same 500 kHz sampling rate. The voltage transient following the arc fault is detectable only by the HBM-based DAQ measurement system due to the high-frequency bandwidth (25 MHz) of the voltage sensor used. The voltage sensor used with the cRIO measurement system having a limited bandwidth from DC to 15 kHz is not able to appropriately reflect the voltage transient.

Other surge signal characteristics such as the rate-of-rise and pulse duration were estimated for different sampling rates of the measurement system, and are presented in Fig. 9. The rate-of-rise is calculated between the 10% and 90% of the reference signal value according to IEEE Std 181-2011 [23], whereas the pulse duration as the time interval between the two 50% reference signal values of the leading edge and the trailing edge of the surge.

The signal characteristics reported are for nine surges acquired at the indicated sampling rate following DC series arcs created under the same mechanical, electrical and environmental conditions. Although little variability may still exist when repeating experiments, the two curves presented in Fig. 9 clearly indicate the dependency of the estimated signal characteristics to the sampling frequency of the measurement system. Both the rate-of-rise and pulse duration parameters follow an exponential change (in contrast to the almost linear relationship of the peak voltage with the sampling rate). They significantly increase above and below the 2 MHz sampling rate point, respectively. The jump in the rate-of-rise curve at 5 MHz sampling frequency, is caused by the natural resonant frequency of the sensor (experimentally quantified around 5 MHz) excited by the arcing phenomenon.

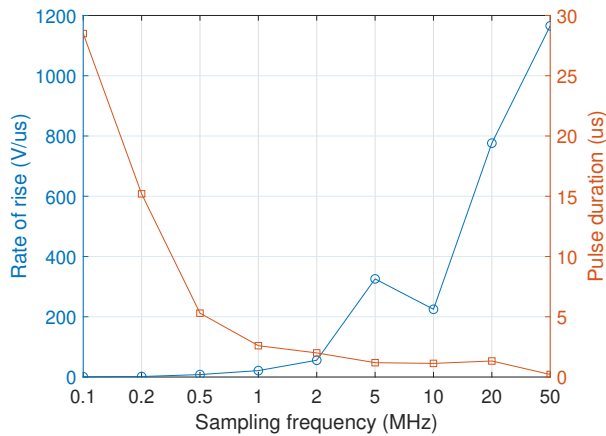These results indicate that although few kHz (typically 5

Fig. 9: Rate of rise and pulse duration as a function of different sampling rates

kHz to 10 kHz) sampling rates and sensor bandwidths may be enough to characterise slow and small varying magnitudes of certain PQ phenomena, higher sensor bandwidths and sampling rates (typically 5 MHz to 10 MHz) are needed to detect and assess disturbances that experience large variations from their steady-state conditions, for example, to provide a complete investigation and appreciation of the surges and consequently their impact on the electrical insulation systems or on the PQ indices.

V. Conclusions

This paper has presented experimental results of voltage transient disturbances present in the LV AC microgrid and in a laboratory-scale DC system equipped with an arc fault generator detected from two measurement systems featuring different bandwidths and sampling rates.

Results indicate that unknown high-frequency disturbances of significant magnitude exist in actual signals. Up to 41 V peak-to-peak repetitive high-frequency voltage transients were found superimposed on a 230 V AC sinusoidal signal, and voltage transients achieving magnitudes of more than 600% of the system voltage have been detected on the considered DC system with maximum voltage, rate-of-rise, and pulse duration characteristics very much affected by the sampling rates used.

The high-frequency detected signals shown in this study have the potential to impact the PQ and impose additional stress on the state of the electrical insulation of electrical equipment and systems. Therefore, it is important to ensure signals are measured with appropriate sample rates and sensor bandwidths to make sure that signals and the impact of high-frequency phenomena, for example, on electrical insulation, can be better quantified and understood.

Acknowledgment

References

[1] A. Ferrero, "Measuring electric power quality: Problems and perspectives," *Measurement*, vol. 41, no. 2, pp. 121–129, 2008. Advances in Measurements of Electrical Quantities.

[2] J. Barros, M. de Apráiz, and R. I. Diego, "Power Quality in DC Distribution Networks," *Energies*, vol. 12, no. 5, p. 848, 2019.

[3] M. H. Bollen, "Understanding power quality problems," in *Voltage sags and Interruptions*, IEEE press, 2000.

[4] Y. Seferi, P. Clarkson, S. M. Blair, A. Mariscotti, and B. G. Stewart, "Power quality event analysis in 25 kv 50 hz ac railway system networks," in *2019 IEEE 10th International Workshop on Applied Measurements for Power Systems (AMPS)*, pp. 1–6, 2019.

[5] Y. Seferi, S. M. Blair, C. Mester, and B. G. Stewart, "Power quality measurement and active harmonic power in 25 kv 50 hz ac railway systems," *Energies*, vol. 13, no. 21, 2020.

[6] A. Arshad and B. G. Stewart, "Modelling harmonic propagation in hvdc system power cables," in *IEEE Electrical Insulation Conference 2021*, 2021.

[7] S. Bahadoorsingh and S. M. Rowland, "The role of power quality in electrical treeing of epoxy resin," in *2007 Annual Report - Conference on Electrical Insulation and Dielectric Phenomena*, pp. 221–224, 2007.

[8] C. Pacheco, J. de Oliveira, and A. Vilaca, "Power quality impact on thermal behaviour and life expectancy of insulated cables," in *Ninth International Conference on Harmonics and Quality of Power. Proceedings (Cat. No.00EX441)*, vol. 3, pp. 893–898 vol.3, 2000.

[9] P. M. Donohue and S. Islam, "The effect of nonsinusoidal current waveforms on electromechanical and solid-state overcurrent relay operation," *IEEE Transactions on Industry Applications*, vol. 46, no. 6, pp. 2127–2133, 2010.

[10] A. Benjamin and S. K. Jain, "A review of literature on effects of harmonics on protective relays," in *2018 IEEE Innovative Smart Grid Technologies-Asia (ISGT Asia)*, pp. 407–412, IEEE, 2018.

[11] C. Muscas, "Power quality monitoring in modern electric distribution systems," *IEEE Instrumentation Measurement Magazine*, vol. 13, no. 5, pp. 19–27, 2010.

[12] G. Rietveld, D. Hoogenboom, and M. Acanski, "Conducted emi causing error readings of static electricity meters," in *2018 Conference on Precision Electromagnetic Measurements (CPEM 2018)*, pp. 1–2, 2018.

[13] R. Quijano Cetina *et al.*, "Energy metering integrated circuit behavior beyond standards requirements," *Energies*, vol. 14, no. 2, p. 390, 2021.

[14] J. Yaghoobi *et al.*, "Impact of high-frequency harmonics (0–9 khz) generated by grid-connected inverters on distribution transformers," *International Journal of Electrical Power & Energy Systems*, vol. 122, p. 106177, 2020.

[15] G. Singh *et al.*, "Impact of high frequency conducted voltage disturbances on led driver circuits," in *2017 IEEE Power & Energy Society General Meeting*, pp. 1–5, IEEE, 2017.

[16] Y. Li *et al.*, "Thermal analysis of metallized film capacitors used in motor drive controller," in *2019 22nd International Conference on Electrical Machines and Systems (ICEMS)*, pp. 1–4, IEEE, 2019.

[17] T. Jiang *et al.*, "Partial discharge activities of pressboard/oil insulation under ac plus dc voltages," in *2013 IEEE International Conference on Solid Dielectrics (ICSD)*, pp. 267–270, IEEE, 2013.

[18] L. Zhu *et al.*, "Electrical tree characteristics in polypropylene under impulse superimposed dc voltage in ln 2," *IEEE Transactions on Applied Superconductivity*, vol. 29, no. 2, pp. 1–3, 2019.

[19] Y. Murata, S. Katakai, and M. Kanaoka, "Impulse breakdown superposed on ac voltage in xlpe cable insulation," *IEEE Transactions on Dielectrics and Electrical Insulation*, vol. 3, no. 3, pp. 361–365, 1996.

[20] G. Van den Broeck *et al.*, "A critical review of power quality standards and definitions applied to dc microgrids," *Applied energy*, vol. 229, pp. 281–288, 2018.

[21] J. Barros, M. De Apráiz, and R. I. Diego, "Definition and measurement of power quality indices in low voltage dc networks," in *2018 IEEE 9th International Workshop on Applied Measurements for Power Systems (AMPS)*, pp. 1–5, IEEE, 2018.

[22] "IEC TR 63282:2020 LVDC systems — Assessment of standard voltages and power quality requirements," 2020.

[23] "IEEE Standard for Transitions, Pulses, and Related Waveforms," *IEEE Std 181-2011*, 2011.